

Mid-crustal fluid mixing in a Proterozoic Fe oxide–Cu–Au deposit, Ernest Henry, Australia: Evidence from Ar, Kr, Xe, Cl, Br, and I

M.A. Kendrick^{a,*}, G. Mark^b, D. Phillips^a

^a Predictive Mineral Discovery Cooperative Research Centre (pmd^{*}CRC), The School of Earth Sciences, The University of Melbourne, Victoria 3010, Australia

^b Predictive Mineral Discovery Cooperative Research Centre (pmd^{*}CRC), The School of Geosciences, Monash University, Victoria 3800, Australia

Received 15 May 2006; received in revised form 15 December 2006; accepted 22 December 2006

Available online 19 January 2007

Editor: R.W. Carlson

Abstract

Fluid inclusions in six quartz veins associated with Cu–Au mineralisation at the giant Ernest Henry iron oxide–copper–gold deposit (167 Mt 1.1% Cu, 0.54 ppm Au) in northwest Queensland, have been analysed for naturally occurring and neutron produced noble gas isotopes of Ar, Kr and Xe.

A combination of thermal and mechanical decrepitation methods enables distinction between four types of fluid inclusion. Ultra-high-salinity (~30 to 70 wt. % NaCl eq.) fluid inclusions have compositions that define two end-members that are variably mixed in different samples. The first end-member has a $^{40}\text{Ar}/^{36}\text{Ar}$ value of ~29,000, a $^{40}\text{Ar}_E/\text{Cl}$ value of $\sim 3 \times 10^{-3}$ and mantle-like Br/Cl and I/Cl values of $1\text{--}2 \times 10^{-3}$ and $\sim 11 \times 10^{-6}$, respectively. The second end-member has a much lower $^{40}\text{Ar}/^{36}\text{Ar}$ value of less than 2500, a $^{40}\text{Ar}_E/\text{Cl}$ value of $\sim 10^{-6}$, low Br/Cl values of $\sim 0.4 \times 10^{-3}$ and I/Cl values of $1\text{--}2 \times 10^{-6}$ (all ratios are molar). Carbon dioxide and later, lower salinity liquid-vapour fluid inclusions have similar $^{40}\text{Ar}/^{36}\text{Ar}$ values of less than ~2500 in all samples.

These data are compatible with genetic models in which Cu–Au mineralisation formed at a depth of 6–10 km, from circulation of magmatic fluids derived from regionally abundant ‘A-type’ granites and a high salinity halite dissolution brine generated from sedimentary formation waters in the upper crust. The largest source of CO₂ was probably carbonate-rich lithologies in the mid-crust. Later, lower salinity fluids with a surficial origin diluted the mineralising brines and are preserved in the latest, secondary fluid inclusions.

These data provide insight on the composition of crustal fluids during the Proterozoic. Furthermore, the magmatic fluid end-member, derived from melts generated by re-melting lower-crustal Paleoproterozoic igneous rocks with a mantle source, preserves mantle-like Br/Cl and I/Cl. These geochemical characteristics are interpreted to provide insight on I-recycling at subduction zones and the composition of seawater in the Paleoproterozoic.

© 2007 Elsevier B.V. All rights reserved.

Keywords: Noble gases; Halogens; Ar–Ar; Quartz; Mt Isa Inlier; Fluid inclusions

1. Introduction

The Cloncurry minerals district of the Mt Isa Inlier is host to a remarkable number of ore deposits that formed

* Corresponding author. Tel.: +61 3 8344 7978; fax: +61 3 8344 7761.
E-mail address: mark.kendrick@unimelb.edu.au (M.A. Kendrick).

during, or prior to, the ~1.5–1.6 Ga Isan Orogeny [1–3]. Ernest Henry which formed at a crustal depth of 6–10 km, is the largest of several iron oxide–copper–gold (IOCG) deposits (Fig. 1), and is considered representative of the deposit class [3,5,6]. IOCG deposits like Ernest Henry comprise breccia-hosted iron oxide (haematite and magnetite) and Cu sulphides, and are enriched in trace elements such as Au, U, and REE [7]. This deposit type is typically associated with regionally extensive pervasive albitic and potassic alteration and mineralisation is commonly localized along fault splays

off major structures [7–10]. Therefore, these alkaline alteration and ore systems provide evidence for lateral fluid flow over 10–100's km and vertical fluid flow of up to ~10 km during orogenesis [7–9,11].

Fluid inclusions within Cu–Au mineralisation stage quartz veins at Ernest Henry preserve the K-rich, sodic ore fluids locally responsible for breccia-hosted IOCG mineralisation [5,12]. These fluids typically include ultra-high-salinity (<70 wt.% NaCl eq.) brines and liquid carbon dioxide, as well as later, lower salinity brines [5,13–16]. The principal controversy in understanding

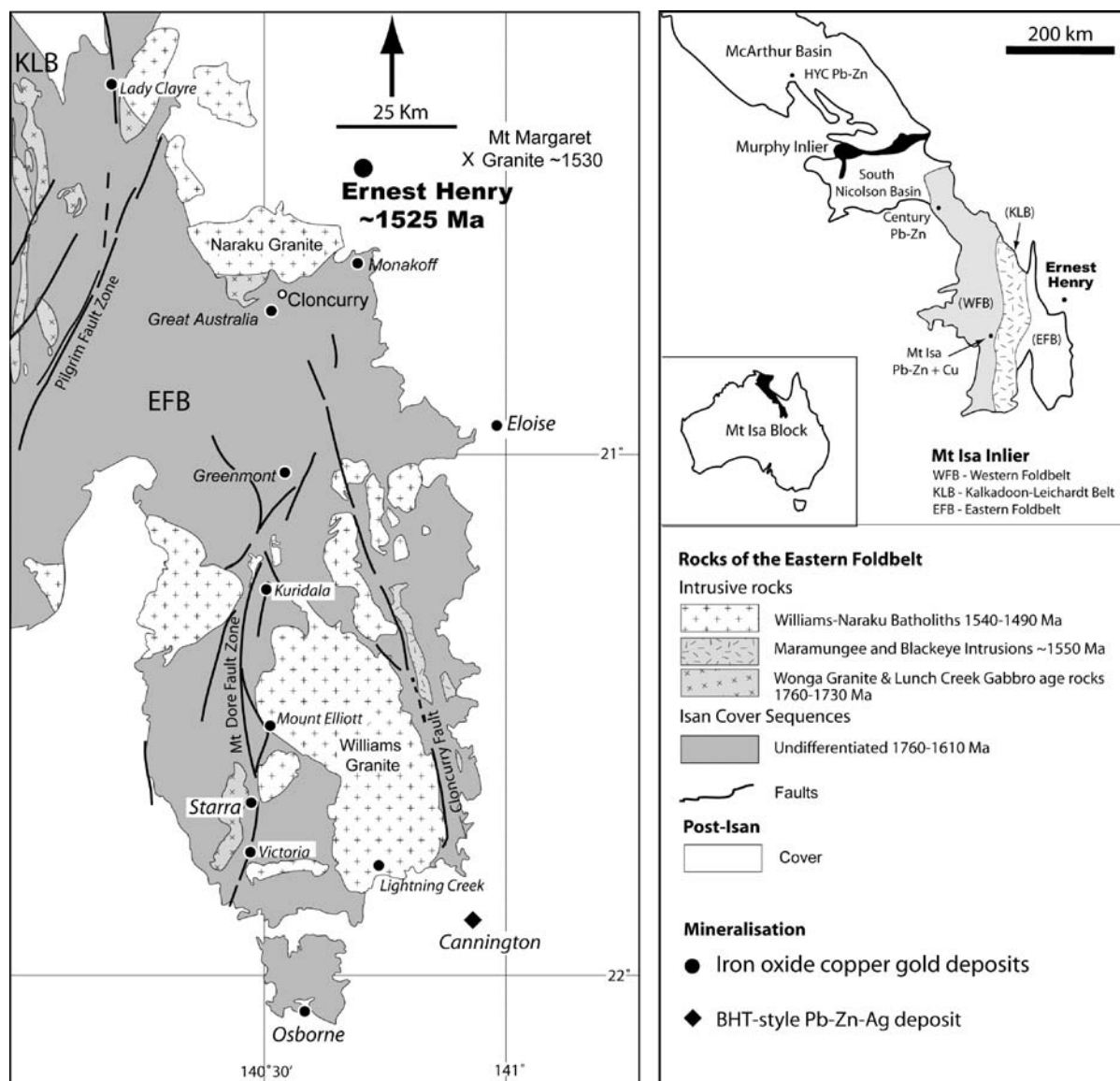


Fig. 1. Locality map indicating the position of IOCG within the Eastern Fold Belt of the Mt Isa inlier, NE Australia. Ernest Henry is the largest IOCG at 167 Mt at 1.1% Cu and 0.54 ppm Au and is ~15 km distant from the Mt Margaret granite which has U–Pb zircon ages of 1530 ± 8 Ma and 1528 ± 6 Ma [4].

IOCG genesis, as well as that of regional alteration, relates to the origin of these diverse fluids. IOCG terranes are commonly associated with both extensive coeval igneous activity and voluminous halite- or scapolite-calcite-bearing sedimentary or meta-sedimentary rocks [7]. Therefore, ultra-high-salinity fluids and carbon dioxide could be attributed to either (1) primary magmatic sources [3,10,17], (2) convective circulation of formation waters with dissolution of halite [8], or (3) metamorphic devolatilisation of Cl-rich scapolite and calcite [7].

In this study, the noble gases (Ar, Kr, Xe) and halogens (Cl, Br, I) have been released from aqueous and carbonic fluid inclusions using a semi-selective thermal decrepitation procedure that allows partial deconvolution of chemical signatures associated with the different fluid types [15]. The halogens are strongly fractionated by interaction with halite, which preferentially excludes Br and I, such that surface-derived halite dissolution waters are expected to have low Br/Cl plus I/Cl values [18,19], and $^{40}\text{Ar}/^{36}\text{Ar}$ values of ~ 300 –2000, similar to other sedimentary formation waters [20,21]. Deeply derived magmatic fluids are expected to have a limited range of Br/Cl and I/Cl [22,23] with elevated $^{40}\text{Ar}/^{36}\text{Ar}$ values of up to $\sim 44,000$ in juvenile fluids [24,25] (or even higher if derived from ancient crust). In addition, the noble gases and halogens can provide some information on metamorphic processes: prograde fluids formed by devolatilisation of crystalline basement are likely to have high (magmatic-like) $^{40}\text{Ar}/^{36}\text{Ar}$ values, low ^{36}Ar concentrations and low salinity (e.g. <20 wt. % [26,27]). Whereas lower $^{40}\text{Ar}/^{36}\text{Ar}$ values (i.e. <2000) could be produced by devolatilisation of ^{36}Ar -rich sedimentary (or meta-sedimentary) rocks. In addition, at low water-rock ratios the fluids' salinity, ^{36}Ar concentration and Br/Cl values could all be elevated by hydration reactions [26,28,29].

The data presented in this study allow new insight of noble gas and halogen systematics in Mesoproterozoic mid-crustal environments and provide a novel way to test the disparate origins suggested for aqueous and carbonic fluids in the IOCG deposit class.

2. Geology and samples

2.1. Regional metamorphism and magmatism

Peak metamorphism in the Eastern Fold Belt of the Mt Isa Inlier occurred synchronously with E–W shortening (D_2) and reached greenschist to upper-amphibolite facies at 1595–1575 Ma [30]. Meta-sedimentary rocks include the 1760–1720 Ma evaporite-rich calc-silicate supracrustal rocks of the Corella

Formation and equivalents (cover sequence 2) as well as the younger 1680–1650 Ma siliclastic-rich rocks of the Soldiers Cap Group (cover sequence 3) [4,31]. Pegmatitic veins were produced in the highest-grade zones [30] close to the ~ 1595 Ma Osborne IOCG [32] and the Cannington Ag–Pb–Zn deposits (Fig. 1) [33].

The regionally extensive Williams–Naraku Batholiths intruded older granitoids and supracrustal rocks during two phases of post-peak-metamorphic magmatism (Fig. 1) [4]. Granodiorite–tonalite–trondhjemite suite intrusions were emplaced close to the Cloncurry Fault (Fig. 1) around ~ 1550 Ma [4,34,35], followed by intrusion of the volumetrically most abundant phases of the Williams–Naraku Batholiths at 1540–1490 Ma (Fig. 1) [4,36,37]. These late- to post- D_3 intrusive rocks have extremely variable compositions [34,38], with the more mafic units including hornblende-diopside monzonites and quartz diorites. The more dominant felsic units with 65–77 wt.% SiO_2 , include K-rich porphyritic monzodiorite, monzogranite, granodiorite and granite [34,35].

The younger granitoids probably formed in an intra-continental/back arc setting and have been variably classified as I- or A-type [4,34–36]. Melt generation is considered to have taken place at a depth of ≤ 25 –30 km in the plagioclase stability field [34,35], and may have been triggered by the introduction of mantle melts in a mafic underplate [4,35,38–40]. At the current level of exposure, some of the mafic units may have had a juvenile origin, but the dominant felsic units recycled Paleoproterozoic igneous rocks with depleted mantle Sm–Nd model ages of ~ 2.2 –2.3 Ga [4,35,37].

2.2. Hydrothermal alteration and mineralisation

Regionally extensive Na–Ca hydrothermal alteration (albitisation) took place at 300–500 °C and is associated with veins that comprise albitic plagioclase, magnetite, clinopyroxene, and amphibole [9,41]. Na–Ca altered rocks occur throughout the Eastern Fold Belt, but are most intensely developed in calc-silicate rocks and along breccia zones in large faults [9,11,42,43]. Na–Ca alteration took place in several discrete episodes and is overprinted by IOCG mineralisation in each of the ore systems [3]. However, at Ernest Henry Na–Ca alteration has a U–Pb titanite age that is indistinguishable to that of pre-ore potassic alteration and intrusion of the 15 km distant Mt Margaret granite at ~ 1525 Ma (Fig. 1) [4,6]. Similar U–Pb titanite ages of ~ 1520 –1530 Ma at several other localities in the Eastern Fold Belt suggest that Na–Ca alteration was widespread at this time [9,44].

The Ernest Henry ore-body is hosted by K-feldspar altered meta-andesitic rocks, interpreted to be temporal

equivalents of the ~1740 Ma Mt Fort Constantine Volcanics [4,6], and minor intercalated meta-sedimentary rocks in a zone of dilation between two shear zones [5,6]. The main Cu–Au ore-forming event (stage 1) is associated with a matrix-supported hydrothermal breccia. Rounded to sub-rounded clasts (5–20 mm) are supported by a matrix of magnetite, calcite, pyrite, biotite, chalcopyrite, K-feldspar, titanite, quartz and diverse accessory phases. Stage 2 veins transect the ore breccias and are mineralogically identical to stage 1 breccia matrix but with calcite, quartz, K-feldspar, chalcopyrite, barite and magnetite more dominant [5,6]. Stable isotope ($\delta^{18}\text{O}$ and $\delta^{34}\text{S}$) values calculated for the ore fluids from mineral analyses are similar to igneous values, compatible with either a magmatic fluid or a sedimentary formation water (cf. [3,5,10]).

2.3. Quartz samples

Six samples, representative of stage 2 quartz veins and associated with the highest grade of Cu–Au mineralisation, were selected from drill core intersections at the centre of the deposit (drill holes; EH205; EH461; EH477; EH501; EH502; see Appendix A). Although high purity separates were obtained by hand picking 1–2 mm quartz grains under a binocular microscope, some of the fluid inclusion wafers contained micron-sized mineral impurities that could not be separated and were associated with late fractures in sample AO424-13.

The fluid inclusion assemblages within the selected samples are typical for stage 2 quartz veins from the Ernest Henry deposit (G. Mark, unpublished data; [16]), and to those reported for other IOCG deposits in the region e.g. [14,45,46]. The relative proportions of ultra-high salinity multi-solid (MS), liquid-vapour-daughter (LVD), liquid-vapour (LV) and liquid carbon dioxide (CO_2) fluid inclusions are given in Table 1. MS and LVD fluid inclusions have typical homogenization temperatures of between ~250 and 550–600 °C corresponding to a large range in salinity (Table 1). LV fluid inclusions have variable final melting temperatures indicating salinities of <5 to ~30 wt.% total dissolved solids. All of these aqueous fluid inclusions can have first melting temperatures as low as –55 °C, indicating a Ca-rich composition, and vapour disappearance usually occurs between ~100 and 200 °C. Carbon dioxide fluid inclusions have melting points of close to –56.6 °C indicating a high purity. CO_2 -fluid inclusions homogenize into the liquid phase between –8 and +25 °C, indicating a range of densities close to those reported for similar deposits, ~0.7–1 g cm^{–3} [45,46].

Table 1
Fluid inclusion types and salinities

Sample	MS 		LVD 		LV 	CO ₂ 
	Freq.	Wt.% NaCl eq.	Freq.	Wt.% NaCl eq.	Freq.	Freq.
AO424-28	16%	51 40–69	4%	35 30–43	75%	5%
AO424-31	9%	51 35–65	16%	33 26–46	70%	5%
AO422-09	6%	49 36–69	4%	51 39–61	70%	20%
AO425-05	7%	46 34–59	13%	36 31–46	60%	20%
AO424-13	14%	41 34–58	6%	33 30–35	70%	10%
AO427-10	2%	39 38–39	13%	35 31–39	65%	20%

Fluid inclusion types: MS—multi solid; LVD—liquid-vapour daughter; LV—liquid-vapour; CO_2 —liquid CO_2 .

Samples listed in order of decreasing fluid inclusion assemblage mean salinity. The salinity mean and range are given for MS and LVD fluid inclusions.

The largest CO_2 fluid inclusions decrepitated at the lowest temperatures of ~200–400 °C, while some regularly shaped smaller CO_2 fluid inclusions persisted to 600 °C. Most aqueous fluid inclusions decrepitated in the range ~250–600 °C, but the most saline LVD and MS fluid inclusions were preferentially preserved to high temperatures, with mean decrepitation temperatures of ≥ 400 –500 °C. This decrepitation behaviour is similar to that reported for quartz samples selected from similar deposits and alteration elsewhere in the region [11,15].

3. Noble gas and halogen methodology

High purity quartz separates were irradiated for 150 Megawatt hours in position 5c of the McMaster Nuclear Reactor, Canada; irradiations designated UM#7 on 7th July 2004 and UM#10 on 1st May 2005. The neutron fluence in both irradiations was monitored using Hb3Gr (1072 Ma) [47] and GA1550 (98.8 Ma) [48] flux monitors and the shallower I-Xe standard [49]. J-values had a mean of 0.0175 ± 0.0003 for UM#7; and 0.0187 ± 0.0002 for UM#10. The additional α and β parameters [47,50] had mean values of $\alpha = 0.62 \pm 0.06$, $\beta = 5.2 \pm 0.2$ for UM#7; and $\alpha = 0.55 \pm 0.01$, $\beta = 4.9 \pm 0.3$ for UM#10. The total neutron fluence (fast and thermal) was very similar at $\sim 10^{19}$ neutrons cm^{–2} for each irradiation, but the resonant neutron correction factors [15] were higher in UM#7 (1.5 for Br and 2.0 for I) than in UM#10 (1.3 for Br and 1.7 for I).

Noble gases were extracted from 45–82 mg of each sample included in UM#7 by stepped heating. This enables semi-selective analysis of the different fluid inclusion types in each sample (Table 1), because each type of fluid inclusion has a slightly different range of decrepitation temperature [15]. Furthermore, high-purity

carbon dioxide fluid inclusions do not contain significant halogens. In addition, 28–33 mg of samples AO422-09, AO424-31 and AO427-10 from UM#7 and two larger (185–312 mg) duplicates of samples AO424-31 and AO427-10 irradiated in UM#10, were analysed by combined *in vacuo* crushing and stepped heating of the crushed residue [51]. The extracted gases were purified using hot and cold zirconium aluminum getters and were isotopically analysed using the MAP 215-50 noble gas mass spectrometer at the University of Melbourne.

Chlorine, Br, I, K, Ca and U are determined from the neutron flux and the measured abundance of nucleogenic (and fissionogenic) noble gas isotopes: $^{38}\text{Ar}_{\text{Cl}}$, $^{80}\text{Kr}_{\text{Br}}$, $^{128}\text{Xe}_{\text{I}}$, $^{39}\text{Ar}_{\text{K}}$, $^{37}\text{Ar}_{\text{Ca}}$ and $^{134}\text{Xe}_{\text{U}}$ [15,49]. The Br/Cl and I/Cl values are proportional to the measured $^{80}\text{Kr}_{\text{Br}}$ / $^{38}\text{Ar}_{\text{Cl}}$ and $^{128}\text{Xe}_{\text{I}}$ / $^{38}\text{Ar}_{\text{Cl}}$ values [15]. Minimum analytical uncertainties (1σ) determined from air calibrations are 0.1% for $^{40}\text{Ar}/^{36}\text{Ar}$ ratios but ~ 3 –5% for Kr/Ar and Xe/Ar ratios determined using a combination of two detectors. The total uncertainty (1σ) is estimated as 10% for Br/Cl ratios and 15% for I/Cl ratios, based on the reproducibility of selected samples included in several irradiations. All ratios are molar, but concentrations are given in weight units unless otherwise stated. The analytical protocol is described in detail elsewhere [15].

4. Noble gas and halogen data

4.1. Sample K and Ar–Ar systematics

Most fluid inclusions have molar K/Cl values of 0.04–0.15 (Table 2), determined by *in vacuo* crushing and from stepped heating of uncrushed samples (≤ 500 °C), which preferentially extracts noble gas isotopes from fluid inclusions [51–53]. Higher K/Cl values of greater than 0.5, obtained from some samples at ≥ 550 °C, are attributed to $^{39}\text{Ar}_{\text{K}}$ outgassed from mineral impurities within the quartz matrix.

The maximum K/Cl values are higher for crushed samples than for uncrushed samples (Table 2), because fewer Cl-rich fluid inclusions are present after crushing. As a consequence it is easier to detect minor K-mineral impurities in crushed samples. However, the K concentration is variable within each of the samples for which duplicates were analysed (Table 2; e.g. 46 ppm in AO427-10a vs. 220 ppm AO427-10c), indicating that the K-mineral impurities are heterogeneously distributed through the samples.

4.1.1. Mineral impurity Ar–Ar ages

It was not possible to obtain quartz samples that were both large enough for detailed stepped heating analysis,

and also free of K-mineral impurities (Table 2). As a result, isochron regressions obtained by stepped heating the crushed residues (Fig. 2), do not constrain the time at which primary fluid inclusions were trapped during the ~ 1525 Ma mineralisation event [6,52]. Instead, mineral impurity ages of ~ 1050 – 1250 Ma are obtained (Fig. 2), and are interpreted to relate to cooling of the mineral impurity through a poorly defined closure temperature of ~ 150 – 250 °C [52]. In these cases, $^{40}\text{Ar}_{\text{R}}$ is lost from the mineral impurity into the surrounding fluid inclusions or quartz matrix, but $^{40}\text{Ar}_{\text{R}}$ is not lost from the actual sample [52]. As a result, the samples yield total fusion ages of much older than the preferred 1525 Ma age of mineralisation (Fig. 2; [6]).

In contrast, sample AO424-13 has an anomalously young total fusion age of ~ 227 Ma, and selected extraction steps yield an ‘isochron’ age of ~ 11 Ma (Fig. 2c). In this case, the apparent age cannot be explained by redistribution of $^{40}\text{Ar}_{\text{R}}$ within the sample. Instead, these data indicate either very late growth of a secondary mineral or $^{40}\text{Ar}_{\text{R}}$ loss from the sample. Growth of late-mica is the favoured explanation because this sample has the highest K content of 0.4 wt.% (Table 2), mineral impurities were observed close to fractures in the fluid inclusion wafer, and the fluid inclusions appear identical to the other samples with respect to type, salinity and Ar concentration (Tables 1 and 2).

The complex Ar–Ar systematics outlined above illustrate the importance of identifying the main reservoir of K and Ar in fluid inclusion-bearing samples, and confirm how difficult it can be to date the actual fluid inclusions [52,54]. As in previous studies, the K abundance and K/Cl values are critical parameters that enable the importance of K-mineral impurities to be quantified, even when such (minor) phases are difficult to detect by microscopy [51,52].

4.2. Fluid inclusion Argon compositions

Samples with < 100 ppm K are dominated by fluid inclusion excess $^{40}\text{Ar}_{\text{E}}$ ¹, with the 1525 Ma age-corrected mean $^{40}\text{Ar}/^{36}\text{Ar}$ value being ~ 2 –6% lower than the uncorrected measured value (total fusion $^{40}\text{Ar}/^{36}\text{Ar}$ values; Table 2). Sample AO422-09 with 300–730 ppm K has one of the largest age-corrections of up to 57% (Table 2). Sample AO424-13 contains a significant mineral impurity in late fractures (not fluid inclusions) and we report ^{40}Ar data for extraction steps

¹ Excess $^{40}\text{Ar}_{\text{E}} = ^{40}\text{Ar}$ not attributed to an atmospheric source ($296 \times ^{36}\text{Ar}$) or in situ radiogenic decay of ^{40}K since the time of trapping.

Table 2
Ernest Henry noble gas, halogen, K and U data summary

	$^{40}\text{Ar}/^{39}\text{Ar}$		Total fusion ² (measured)- corrected	$\text{Cl}/^{36}\text{Ar} \times 10^6$		Mean (\pm S.D.)	NaCl (wt%)		^{35}Ar [ppb]	$^{40}\text{Ar}/\text{El}$ (ppm)	F^{36}Kr <i>in vacuo</i> crush range	$\text{Br}/\text{Cl} \times 10^{-3}$ 200–700 °C ⁴ bulk (TF)	$\text{I}/\text{Cl} \times 10^{-6}$ range or (TF)	K/Cl		U (ppb)		
	Max Age- corrected ¹	Max		MS mean (max) ³	MS mean (max)		(wt%)	MS mean (max)										
AO424-28	82	H	6400±1000 3850±180	58±10	119±27	51 (69)	5.4 (7.3)	41 (56)	–	–	1.2–1.6	1.4–3.4	0.06–0.15	3.2±0.2	5.1 (6.9)	68	20	
AO424-31	a	54	H	6730±840 2480±70	207±28	51 (65)	1.5 (1.9)	16 (21)	–	–	0.72–1.3	1.7–2.9	0.04–0.4	0.40±0.02	14 (17)	25	20	
	b	31	C	6780±180 3400±50	51±5	108±27	6.2 (7.8)	38 (48)	0.9–1.3	1.7–2.9	1.3	4.7	0.06–0.12	0.12±0.01	4.1 (5.2)	25	100	
	cH	2330±50		3400±50	56±6	61±73	5.6 (7.1)	21 (27)	–	–	–	–	0.06–0.13	6.1±0.4	4.4 (5.6)	–	–	
	c	195	C	5690±80 2700±10	82±6	62±8	3.8 (4.9)	22 (28)	1.1–1.3	0.8–1.7	1.1	–	0.07–0.09	0.09±0.01	3.1 (3.9)	47	–	
	cH	2920±330		2600±10	137±9	31±17	2.3 (2.9)	11 (14)	–	–	–	–	0.04–0.12	1.5±0.1	4.1 (5.2)	–	–	
AO422-09	a	45	H	2540±140* 1200±10	252±12	10±4	1.2 (1.7)	3.4 (4.7)	–	–	–	–	0.36–1.0	0.58–1.5	3.8±0.2	4.6 (6.5)	730	2
	b	33	C	1820±10 1010±10	165±8	9.3±0.5	1.8 (2.6)	3.1 (4.4)	1.0–1.4	1.6–2.3	0.53	1.1	0.03–0.08	0.079±0.004	2.6 (3.7)	300	10	
	cH	1500±220		760±5	135±20	6.5±3.3	2.2 (3.1)	2.2 (3.1)	–	–	–	–	0.01–0.44	9.2±0.4	14.4 (20)	–	–	
AO425-05	69	H	29,000±8000 11,800±500	87±23	350±70	46 (59)	3.3 (4.2)	110 (141)	–	–	–	–	1.3–2.0	0.04–0.22	0.22±0.02	7.2 (10)	14	6
AO424-13	75	H	3460±50 1060±40	367±85	43±48	41 (58)	0.7 (1.0)	12 (17)	–	–	–	–	0.60–1.1	0.82–1.6	0.05–0.09	243±5	3700	70
AO427-10	a	58	H	9500±360 4120±130	530±32	34±38	0.5 (0.6)	9.1 (12)	–	–	–	–	0.37–0.60	1.6–4.0	0.19±0.01	4.4 (5.7)	46	40
	b	28	C	15,770±960* 3490±30	448±34	38±7	0.5 (0.7)	10 (13)	1.1–3.8	1.4–5.1	0.45	1.9	0.03–0.07	0.065±0.003	1.8 (2.3)	51	50	
	c	312	C	6900±100 3780±10	270±18	30±4	0.9 (1.1)	8.0 (10)	–	–	–	–	0.05–0.06	0.060±0.004	1.6 (2.0)	220	–	
	cH	7260±50		375±25	14±9	14±9	0.6 (0.8)	3.7 (4.8)	–	–	–	–	0.06–0.11	3.5±0.2	2.9 (3.7)	–	–	

Reference values⁷
 Meteoric 295.5
 Mantle fluids ~44,000

All ratios are molar.

¹ Age-corrected (1525 Ma) sample maximum $^{40}\text{Ar}/^{39}\text{Ar}$ values. Max values include data obtained in the temperature range 200–1600 °C or by *in vacuo* crushing. The asterisk * indicates $^{40}\text{Ar}/^{39}\text{Ar}$ values that may be unrepresentatively high due to intra-sample ^{40}Ar redistribution [52].

² Uncorrected-measured and age-corrected (1525 Ma) sample mean (total fusion) $^{40}\text{Ar}/^{39}\text{Ar}$ values.

³ MS = multi-solid fluid inclusions. The concentration of Ar and K in MS fluid inclusions is calculated from the mean and maximum salinity of MS fluid inclusions, the tabulated $\text{Cl}/^{36}\text{Ar}$ and $^{36}\text{Ar}/\text{Cl}$ values and the upper limit of the range of fluid inclusion K/Cl values. Precision is limited to ~30% by the variable nature of the sample material.

⁴ The range of Br/Cl and I/Cl values in the temperature ranged considered most representative of the fluid inclusions is given for uncrushed samples [15]. A bulk or total fusion (TF) value is given for samples analysed by combined *in vacuo* crushing and stepped heating of the crushed residue.

⁵ FI = fluid inclusion value estimated for K/Cl by *in vacuo* crushing or stepped heating at ≤500 °C.

⁶ The accuracy of sample K concentration (FI + matrix) is limited by calibration of mass spectrometer sensitivity to ~20 % and is given to two significant figures, sample U concentrations are only semi-quantitative and are given to the nearest 10 or whole number.

⁷ Reference values in [23–25,49,55].

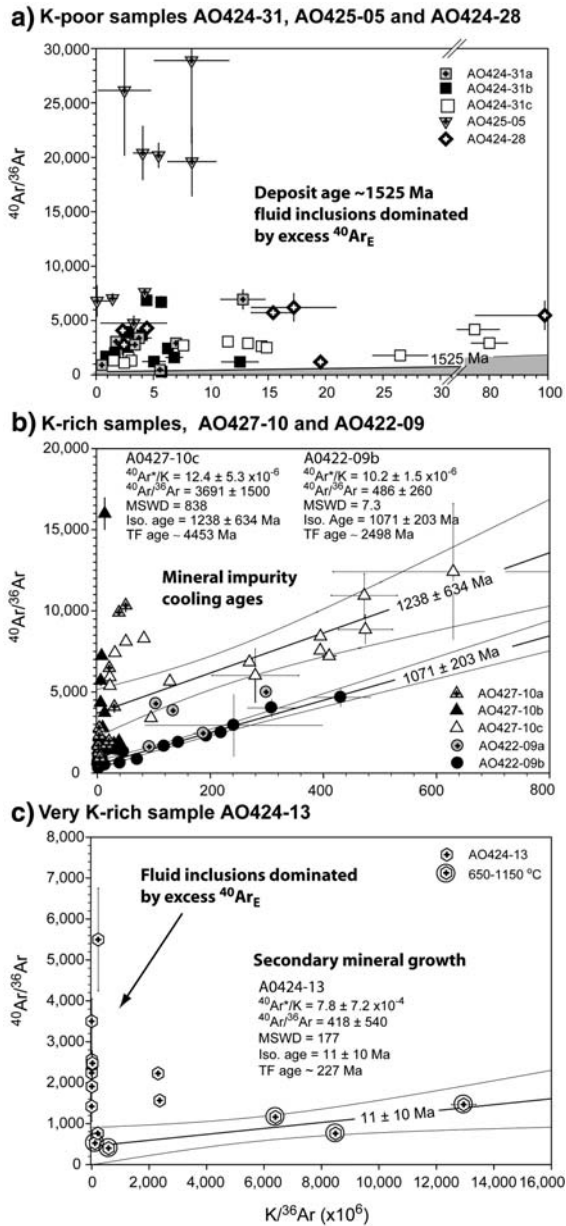


Fig. 2. Isochron diagrams for the Ernest Henry quartz samples. (a) Samples with total K of 14–68 ppm and max K/Cl of 6.1 (Table 2) are dominated by excess $^{40}\text{Ar}_E$. The preferred deposit age of ~1525 Ma [6] is shown for reference. (b) Samples AO427-10 and AO422-09 with 50–700 ppm K and maximum K/Cl values of >9 (Table 3) yield mineral impurity cooling ages. (c) Sample AO424-13 with ~0.4 wt.% K (Table 2), contains fluid inclusions dominated by excess $^{40}\text{Ar}_E$, but the mineral impurity yields an age of ~11 Ma. Abbreviations—Iso. Age = ‘isochron’ age, TF age = total fusion age. The measured $^{40}\text{Ar}/^{36}\text{Ar}$ values are not age-corrected in this plot.

at ≤ 500 °C only. The mineral impurity is not degassed at these temperatures and the corresponding age correction is $\leq 10\%$ (Table 2). It is noteworthy that

sample AO425-05 with the highest $^{40}\text{Ar}/^{36}\text{Ar}$ value has a very small age correction (Table 2), demonstrating that variation in fluid inclusion $^{40}\text{Ar}/^{36}\text{Ar}$ is not attributed to radiogenic $^{40}\text{Ar}_R$ in growth.

Unless otherwise indicated, the reported $^{40}\text{Ar}/^{36}\text{Ar}$ values (from here in) are age-corrected and representative of the initial, 1525 Ma, fluid inclusion compositions (Table 2). As fluid inclusion leakage is not required to explain any of these data, and it has been demonstrated that quartz fluid inclusions are retentive of Ar over billions of years [52], chemical parameters that exclude ^{40}Ar (Br/Cl, I/Cl, Cl/ ^{36}Ar , ^{36}Ar concentration, etc.) are representative of IOCG fluids in every sample.

4.2.1. Deconvolving MS, LVD, LV and CO_2 fluid inclusions

The Ar-isotope data for each sample define a mixing array in age-corrected $^{40}\text{Ar}/^{36}\text{Ar}$ vs. Cl/ ^{36}Ar space, and Cl is strongly correlated with $^{40}\text{Ar}_E$ in samples AO427-10, AO425-05, AO424-28 and AO424-31 (Fig. 3). In these cases, extraction steps with the highest Cl/ ^{36}Ar and $^{40}\text{Ar}/^{36}\text{Ar}$ values are most representative of the highest salinity MS and LVD fluid inclusions [23]. Conversely, extraction steps with lower Cl/ ^{36}Ar values are more representative of lower salinity LV or CO_2 fluid inclusions which are inferred to have the lowest $^{40}\text{Ar}/^{36}\text{Ar}$ values (Fig. 3). MS and LVD fluid inclusions in sample AO425-05 have a $^{40}\text{Ar}/^{36}\text{Ar}$ value of ~29,000, which is higher than seen in similar fluid inclusions in any other sample (Fig. 3). In contrast, the CO_2 and LV fluid inclusions in this sample could be

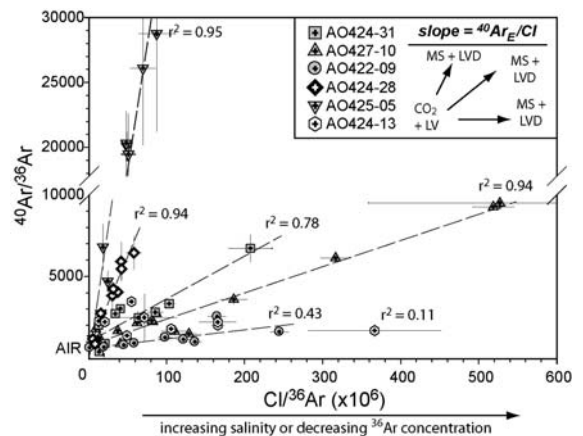


Fig. 3. Age-corrected (1525 Ma) $^{40}\text{Ar}/^{36}\text{Ar}$ vs. Cl/ ^{36}Ar for Ernest Henry Quartz. Data points for samples AO425-05, AO424-28, AO424-31, and AO427-10 are strongly correlated with the slopes approximating the average $^{40}\text{Ar}_E/\text{Cl}$ value (Table 2). CO_2 and LV fluid inclusions have low Cl/ ^{36}Ar and $^{40}\text{Ar}/^{36}\text{Ar}$ values (see schematic inset by legend). Nb—in the interests of clarity a single split (split-a) is shown for each sample.

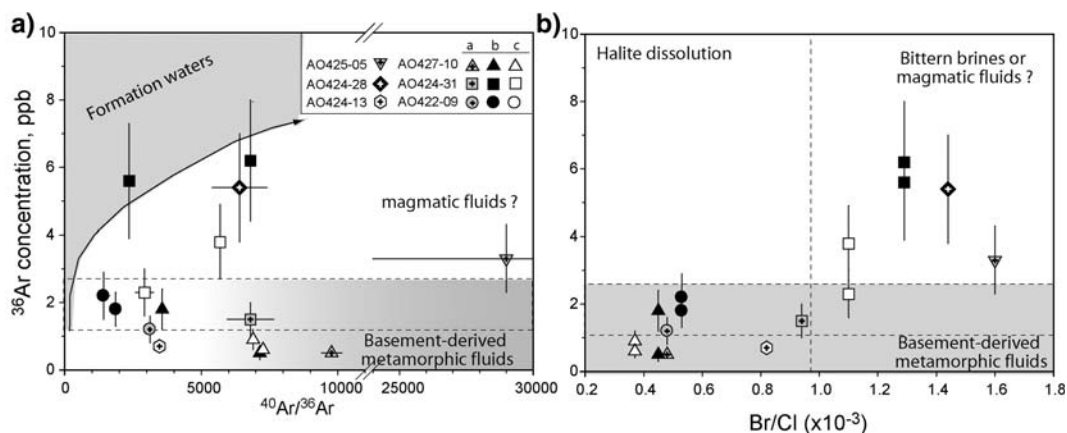


Fig. 4. ^{36}Ar concentration of MS fluid inclusions (a) as a function of the maximum age-corrected $^{40}\text{Ar}/^{36}\text{Ar}$ (1525 Ma) and (b) sample mean Br/Cl (data from Table 2). Sedimentary formation water and basement-derived metamorphic fluid fields are shown for reference. The Formation water field in panel a has a lithology dependent slope, but high ^{36}Ar concentrations (>27 ppb) are expected in fluids with high $^{40}\text{Ar}/^{36}\text{Ar}$ values (e.g. >5000) [26]. Basement-derived metamorphic fluids are likely to have ASW or lower ^{36}Ar concentrations (see [26]). ASW=Air Saturated Water (meteoric or seawater) with 1.3–2.7 ppb ^{36}Ar [55] is shown as dotted horizontal lines. Halite dissolution leads to low Br/Cl values. Fluids in AO425-05 have a preferred magmatic origin, see discussion.

similar to CO_2 and LV fluid inclusions in the other samples with maximum $^{40}\text{Ar}/^{36}\text{Ar}$ values of 2400–4700 (the minimum measured values; Fig. 3).

Samples AO422-09 and AO424-13 have maximum $^{40}\text{Ar}/^{36}\text{Ar}$ values of only 1500–2500, and $^{40}\text{Ar}_E/\text{Cl}$ values of $\sim 10^{-6}$ (Fig. 3). Cl is not strongly correlated with $^{40}\text{Ar}_E$ in these samples and some of the highest $^{40}\text{Ar}/^{36}\text{Ar}$ values measured in sample AO424-13 correspond to the lowest $\text{Cl}/^{36}\text{Ar}$ values giving a weakly negative correlation (Fig. 3). In these cases, it is suggested that MS, LVD, LV and CO_2 fluid inclusions all have similar $^{40}\text{Ar}/^{36}\text{Ar}$ values. Alternatively, CO_2 and LV fluid inclusions could have higher $^{40}\text{Ar}/^{36}\text{Ar}$ values than MS and LVD fluid inclusions in sample AO424-13 (but less than ~ 2500 ; Fig. 3).

4.2.2. Kr, Xe and fluid inclusion Ar concentrations

Stepped heating preferentially extracts fissionogenic isotopes of Kr and Xe, indicating that U present at the ppb-level is situated in the quartz matrix not fluid inclusions (Table 2). The $^{84}\text{Kr}/^{36}\text{Ar}$ and $^{129}\text{Xe}/^{36}\text{Ar}$ values obtained by *in vacuo* crushing samples AO427-10bc, AO424-31bc and AO422-09b are reported relative to the atmospheric ratios, as fractionation values ($F^{84}\text{Kr}$ and $F^{129}\text{Xe}$)² (Table 2). Most of these values are intermediate of Air Saturated Water (ASW) and air (Table 2; Appendix), and encompass a similar range as mid-crustal rocks (e.g. [56]). These values are probably representative of mid-crustal

fluids; however, the possibility that a minor atmospheric (air) component with a $^{40}\text{Ar}/^{36}\text{Ar}$ value of 296 is present cannot be eliminated.

If present atmospheric Ar, which could have been introduced in either ancient times or as a modern contaminant, would move all the data points in Fig. 3 variable distances toward air. This would increase the scatter of negatively correlated data points (i.e. AO424-13), but reinforce positive correlations (Fig. 3). However, as each extraction step exhibits variable $^{40}\text{Ar}_E/\text{Cl}$, Br/Cl , I/Cl as well as $^{40}\text{Ar}/^{36}\text{Ar}$ and $\text{Cl}/^{36}\text{Ar}$ values (Fig. 3), the spread of these data cannot be explained by atmospheric contamination alone and any atmospheric component is probably minor.

The ^{36}Ar concentration of high salinity fluid inclusions can be calculated from the mean salinity of MS fluid inclusions and the maximum $\text{Cl}/^{36}\text{Ar}$ value determined for each sample (Table 2). The ^{36}Ar concentration is unrelated to the age-corrected $^{40}\text{Ar}/^{36}\text{Ar}$ value (Fig. 4a), and varies between 0.5 and 6.2 ppb, with the lowest values reported for samples with low Br/Cl values (Fig. 4b). The $^{40}\text{Ar}_E$ concentrations vary from ~ 1 to >100 ppm and the highest values are in samples with elevated $^{40}\text{Ar}/^{36}\text{Ar}$ values (Table 2).

4.3. Fluid inclusion halogen variability

Most samples have fluid inclusion molar Br/Cl values that decrease with increasing temperature and $\text{Cl}/^{36}\text{Ar}$ values that increase with increasing temperature (200 °C to ~ 600 °C; Fig. 5). The increase in $\text{Cl}/^{36}\text{Ar}$ is compatible with the preferential decrepitation of the

² $F X = (X/^{36}\text{Ar})_{\text{sample}} / (X/^{36}\text{Ar})_{\text{air}}$. Air has F -values of 1, meteoric water and seawater in the temperature range 0–20 °C (ASW—Air Saturated Water) have $F^{84}\text{Kr} \sim 1.8$ –2.1 and $F^{129}\text{Xe} \sim 3.1$ –4.2 [55].

most saline MS and LVD fluid inclusions at temperatures of >400 °C (Section 2.3), suggesting that MS and LVD fluid inclusions have some of the lowest Br/Cl values (Fig. 5). The decrease in $\text{Cl}/^{36}\text{Ar}$ above 600 °C is probably explained because less gas is evolved from Cl-rich fluid inclusions at these temperatures [15] making it more susceptible to contamination by minor atmospheric ^{36}Ar .

In two of the three samples for which multiple splits were analysed, the mean Br/Cl and I/Cl values obtained by stepped heating uncrushed samples (200–700 °C) are very close to the bulk (total fusion) values obtained by combined *in vacuo* crushing and stepped heating (200–1600 °C) of the crushed residue (Figs. 4b and 6; Table 2). The different Br/Cl and I/Cl values determined for splits a, b and c of sample AO424-31 indicate real intra-sample variation (Fig. 4b; Table 2; Appendix).

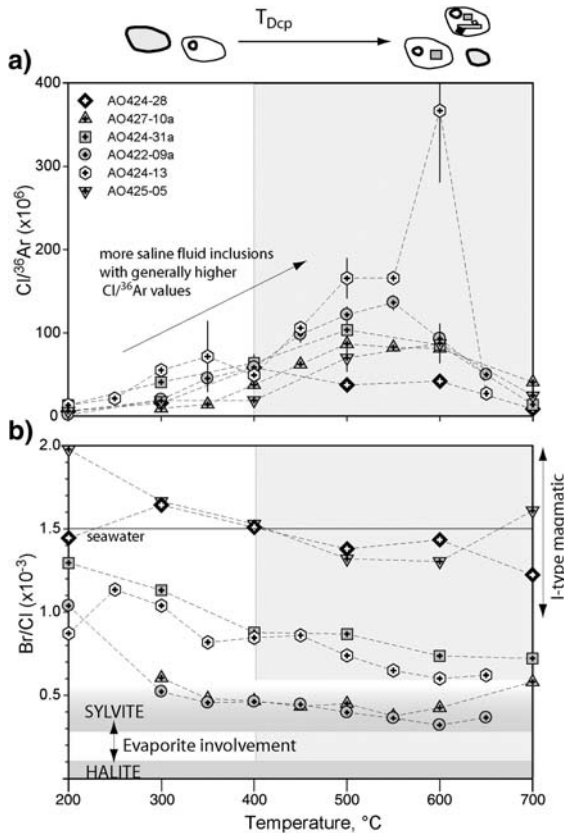


Fig. 5. Composition decrepitation diagrams for Ernest Henry quartz samples. (a) $\text{Cl}/^{36}\text{Ar}$ vs. temperature. MS and LVD fluid inclusions are interpreted to dominate the decrepitation signature between 400 and 700 °C. (b) Br/Cl vs. temperature. The Br/Cl composition of halite and Sylvite have been estimated from the composition of modern day seawater ($\text{Br}/\text{Cl} \sim 1.5 \times 10^{-3}$; [66]) and the Br/Cl partition coefficients for halite (0.033) and sylvite (0.2) [19]. Additional scatter is expected because of Br-rich fluid inclusions or incongruent halite dissolution [67].

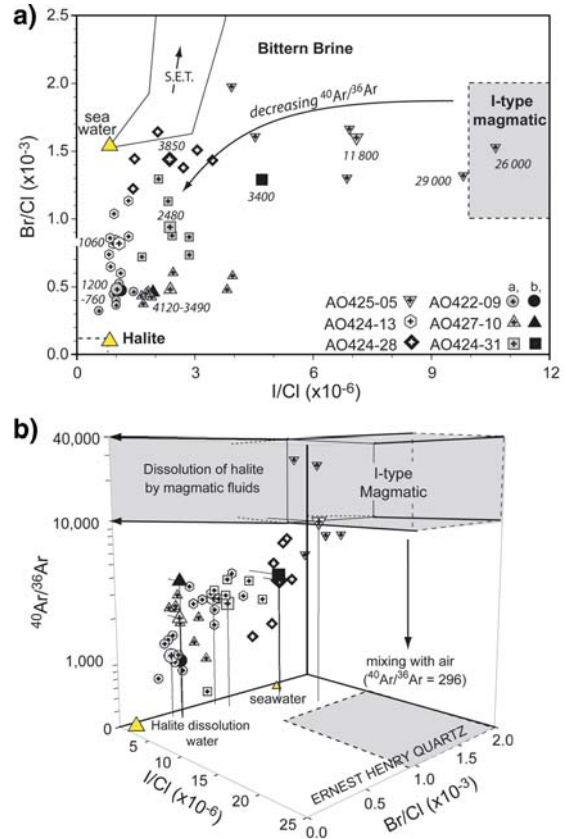


Fig. 6. (a) Br/Cl vs. I/Cl, with mean age-corrected $^{40}\text{Ar}/^{36}\text{Ar}$ values (1525 Ma) given for each sample. (b) 3D multicomponent diagram showing Br/Cl and I/Cl vs. age-corrected $^{40}\text{Ar}/^{36}\text{Ar}$ data (1525 Ma) for Ernest Henry Quartz samples. In both diagrams large symbols represent mean values determined on uncrushed samples (200–700 °C) or bulk (total fusion) values determined by combined *in vacuo* crushing and stepped heating of the crushed residue. Small symbols represent intra-sample variation for uncrushed samples 200–700 °C. The values of seawater, the seawater evaporation trajectory, halite dissolution water (the Hansonburg MVT) and magmatic fluids (based on Porphyry Copper Deposits) are shown for reference, see text [22,23,66,68].

Two of the six samples have fluid inclusion Br/Cl values entirely within the range of $\sim 1\text{--}2 \times 10^{-3}$, that is typical of magmatic fluid inclusions in samples from Porphyry Copper Deposits (PCD) [23] and mantle fluids in diamond [49,57]. However, the majority of I/Cl values are lower than those of magmatic fluids in PCD [23] with only the highest value of 11×10^{-6} determined for sample A0425-05 overlapping the mantle/magmatic range (Fig. 6a; Table 2; [23,49,57]). The remaining samples contain fluid inclusions that are enriched in Cl relative to both Br and I, and the minimum Br/Cl and I/Cl values of 0.36×10^{-3} and $\sim 10^{-6}$ are suggestive of halite dissolution (Fig. 6).

4.3.1. Halogen vs. argon correlations

MS and LVD fluid inclusions in sample AO425-05 with the highest, most ‘magmatic’, Br/Cl and I/Cl values, also have the highest $^{40}\text{Ar}/^{36}\text{Ar}$ values of $\sim 29,000$ (Fig. 6; Table 2). MS and LVD fluid inclusions in samples AO422-09 and AO424-13 with low Br/Cl and I/Cl values have $^{40}\text{Ar}/^{36}\text{Ar}$ values of less than 1500–2500 (Fig. 6).

The spread in these data is interpreted as strong evidence for the involvement of at least two high-salinity fluids, because the order of magnitude decrease in $^{40}\text{Ar}/^{36}\text{Ar}$ is accompanied by a simultaneous decrease the Br/Cl plus I/Cl values (Figs. 4 and 6). The simultaneous change in all of these parameters is unlikely to be explained by dissolution of halite alone, which would preferentially alter the halogen ratios (Fig. 6). It also cannot be explained by other wall rock interactions because the Br/Cl value is unlikely to be fractionated at high water-rock ratios [58]. In addition, wall rock interaction would lead to a correlation between $^{40}\text{Ar}/^{36}\text{Ar}$ and ^{36}Ar concentration (cf. Fig. 4), with the fluid that has undergone the greatest degree of wall rock interaction acquiring the highest ^{36}Ar concentration [26]. Finally, the variations cannot be explained by phase separation, which on the basis of solubility, would strongly fractionate the noble gas elemental ratios but would not affect isotopic compositions [55].

Nonetheless, the relationship between the noble gases and the halogens is clearly complex. Br is not linearly correlated with I and samples AO427-10 and AO422-09, with the equal lowest Br/Cl values have quite different $^{40}\text{Ar}/^{36}\text{Ar}$ values (Table 2; Fig. 6a). Together the total variation in ^{36}Ar concentration, Br/Cl, I/Cl, $^{40}\text{Ar}/^{36}\text{Ar}$ values as well as the lack of any clear correlation between any of these parameters with mean salinity, suggests that multiple fluids or processes shape the geochemical variation (Fig. 6; Table 2 lists samples in order of decreasing fluid inclusion salinity).

5. Discussion

The variation in Ernest Henry noble gas and halogen data has been interpreted to result primarily from mixing of two high-salinity fluids (fluids #1 and #2; Fig. 6). In addition, late lower salinity LV fluid inclusions (fluid #3) and CO_2 fluid inclusions with negligible salinity are present in all of the samples (Table 1; Fig. 3). Stepped heating experiments help resolve these different fluid inclusion types and Cl-poor CO_2 plus LV fluid inclusions are inferred to have uniformly low $^{40}\text{Ar}/^{36}\text{Ar}$ values (Fig. 3). The compositions of the different fluid end-members and the significance of these compositions are summarised in Table 3.

5.1. Fluid #1

The high $^{40}\text{Ar}/^{36}\text{Ar}$ value of $\sim 29,000$ in fluid #1 suggests a deep source from either the basement or the mantle, and could be representative of either a magmatic or a metamorphic fluid. However, the ^{36}Ar concentrations (3–6 ppb) and the salinities (<70 wt.% NaCl eq.), are higher than the values of 1.5–3 ppb ^{36}Ar and <20 wt.% NaCl eq. determined for fluids interpreted to have had a metamorphic-basement origin in the unrelated Mt Isa Cu deposit [26] (Tables 2 and 3). In addition, the Br/Cl and I/Cl values (Table 3) are much lower than those of the interpreted metamorphic fluids at Mt Isa [26].

The mantle-like Br/Cl and I/Cl values of fluid #1 could be explained if a magmatic fluid was: (1) sourced from magmas generated from (mantle-derived) igneous rocks in the lower crust, that preserved mantle-like Br/Cl and I/Cl values; or (2) the magmatic fluid contained a juvenile component. The 1540–1490 Ma magmatism in the Cloncurry District is dominated by ‘A-type’ granites sourced from variably reworked Paleoproterozoic igneous rocks [4,35–37] making the first alternative most likely. However, a juvenile component could be involved if the relatively minor mafic phases of the Williams–Naraku Batholith [35] have a more voluminous expression at depth.

The favoured interpretation of fluid #1 as a magmatic fluid derived from magmas generated by re-melting Paleoproterozoic igneous rocks (i.e. crust), implies that the mantle-like halogen signature was not significantly fractionated during initial separation of the Paleoproterozoic crust from the mantle or during subsequent re-melting/recycling. Such non-fractionation is consistent with the similarity of Br/Cl and I/Cl values reported for MORB, Island Arc Basalts (IAB) and fluid inclusions in some mantle diamond and arc related Porphyry Copper Deposits [23,49,59]. The non-fractionation can be explained if the halogens are quantitatively mobilised during the melting processes that formed all of these rocks and fluids. However, this does not mean that magmas generated in the crust will always yield magmatic fluids with mantle-like Br/Cl and I/Cl compositions. For example, lower Br/Cl values have been reported in ‘magmatic’ fluids associated with the Cornubian Batholith, England [22,60,61].

5.1.1. Comparison with magmatic fluids in Porphyry Copper Deposits

The maximum $^{40}\text{Ar}/^{36}\text{Ar}$ value of 29,000 is almost an order of magnitude higher than the highest values measured in Porphyry Copper Deposits (PCD), that are

Table 3
Summary of fluid types involved in IOCG mineralisation at Ernest Henry

	Fluid #1	Fluid #2	Fluid #3 (late)	CO ₂
$^{40}\text{Ar}/^{36}\text{Ar}$ $^{40}\text{Ar}_{\text{E}}/\text{Cl}$	 ~29,000 3×10^{-3} Deep crustal or mantle, magmatic fluids or, basement-derived metamorphic fluids.	 <2500 10^{-5} to 10^{-6} Similar to sedimentary formation waters or metamorphic fluids derived from sedimentary or meta-sedimentary rocks.	 <1000 – Surficial origin.	 <2500 Crustal origin inferred: CO ₂ provides evidence for ‘minor’ devolatilisation of calc-silicate rocks.
$\left[\frac{^{40}\text{Ar}_{\text{E}}}{^{36}\text{Ar}} \right]$	~100 ppm 3.3–6.2 ppb Enriched in ^{36}Ar and $^{40}\text{Ar}_{\text{E}}$ relative to mantle fluids in diamond or metamorphic fluids derived from the deep crust. Probably representative of magmatic fluids.	0.4–3 ppm 0.5–2.5 ppb Ar concentration similar to or slightly lower than meteoric water. Could indicate a metamorphic source or minor Ar loss from an unevolved sedimentary formation water.	<0.4 ppm ~1.6–2.7 ppb? Assumed to be similar to air saturated water.	? ? Cannot estimate concentrations as CO ₂ fluid inclusions have low abundance and do not contain Cl.
Br/Cl I/Cl Salinity	$1-2 \times 10^{-3}$ $\sim 11 \times 10^{-6}$ <69 wt.% NaCl eq. Similar composition to I-poor mantle fluids. Likely to reflect a source from recycled Paleoproterozoic igneous rocks with an ultimately mantle origin.	$\sim 0.4 \times 10^{-3}$ $\sim 1 \times 10^{-6}$ <69 wt.% NaCl eq. Indicate halite/scapolite dissolution at pressures and temperatures much greater than surface conditions where saturation ≈ 26 wt.% NaCl eq.	Similar to primary fluids? Similar to primary fluids? <5 wt.% NaCl eq. Thought to be a low salinity fluid that dilutes the pre-existing high salinity primary brines and has little effect on halogen composition.	CO ₂ fluid inclusions are not a significant reservoir of the halogens.

All ratios are molar.

less ambiguously related to magmatism [22,23]. This apparent paradox may be explained because most PCD occur at crustal depths of <2 km and exhibit evidence for vigorous fluid boiling with depleted ^{36}Ar concentrations as low as 0.2 ppb; and at Bingham Canyon highly fractionated $F^{84}\text{Kr}$ and $F^{129}\text{Xe}$ values of much greater than ASW [23]. The resulting ^{36}Ar -poor nature of PCD ore fluids, enabled overprinting of the magmatic $^{40}\text{Ar}/^{36}\text{Ar}$ signature by minor contributions of meteoric and/or sedimentary formation water, with low $^{40}\text{Ar}/^{36}\text{Ar}$ values but much higher ^{36}Ar concentrations [23].

In contrast, the Ernest Henry IOCG deposit formed at much deeper crustal levels of 6–10 km [3,5,6]. The hydrothermal brecciation at Ernest Henry is probably related to unmixing of aqueous and CO_2 fluids (Table 1), rather than fluid boiling [17,62]. The fluid inclusion $F^{84}\text{Kr}$ and $F^{129}\text{Xe}$ values are in the range of air and ASW (Table 2) and the ^{36}Ar concentration is up to an order of magnitude higher than in PCD [22,23]. The lack of either Ar-loss or noble gas fractionation at Ernest Henry, implies that either phase separation was less important than in many PCD, or that at depths of 6–10 km, the heavy noble gases (Ar, Kr, Xe) are not strongly fractionated between supercritical CO_2 and aqueous fluids. As a result the primary Ar signature of the magmatic fluid has been better preserved at Ernest Henry (Fig. 6) than in any PCD studied to date [22,23]. In addition, the current results indicate that magmatic fluids in the crust have much higher ^{36}Ar concentration (and salinity) than mantle fluids trapped in African diamond [49].

5.2. Fluid #2 and CO_2

The low $^{40}\text{Ar}/^{36}\text{Ar}$ values of ~1500–2500 in fluid #2 with the lowest Br/Cl and I/Cl values are compatible with a sedimentary formation water that has dissolved halite (Fig. 6b) [8]. Similarly low Br/Cl values have been reported for fluid inclusions in samples from two other Cloncurry District IOCG [15] and some South American IOCG deposits [63].

The Corella Formation comprises meta-evaporitic calc-silicate rocks, and is widely distributed throughout the Cloncurry District. However, these rocks could not have been a source of halite during the ~1525 Ma mineralisation event, because they were originally metamorphosed during peak metamorphism 60–70 Ma earlier [30]. Instead, it is implied that either (1) halite dissolution sedimentary formation waters infiltrated from younger sediments above the present erosion level (e.g. Fig. 7), or (2) the high salinity together with low Br/Cl and I/Cl values, was attained by devolatilisation/dissolution of Cl-rich meta-evaporitic scapolite in the Corella Formation.

The meta-evaporitic scapolite should preserve the low Br/Cl values (and by analogy I/Cl values) of halite because scapolite has a Br/Cl partition coefficient of one [64].

Scapolite breakdown textures are characteristic of the regionally extensive Na–Ca alteration, implying that the scapolite-rich rocks could have been a significant source of ligands, if the fluids responsible for Na–Ca alteration were later involved in IOCG mineralisation (i.e. [8,9]). Metamorphic aureoles are poorly developed around the ~1540–1490 Ma Williams–Naraku Batholiths at the current exposure level [30], but significant metamorphic volatiles could have been released, and drawn down from higher levels of the crust.

The $^{40}\text{Ar}/^{36}\text{Ar}$ data do not conclusively distinguish a possible metamorphic/metasomatic fluid, from a sedimentary formation water, because in contrast to ^{36}Ar -poor crystalline basement rocks, devolatilisation of meta-sedimentary rocks could yield quite low $^{40}\text{Ar}/^{36}\text{Ar}$ values [26]. For example, based on modified forms of the K–Ar decay equation (Eqs. (1) and (2)) the Corella Formation could have had a $^{40}\text{Ar}/^{36}\text{Ar}$ value as low as ~1000–2000 at the 1525 Ma age of mineralisation:

$$\left(\frac{^{40}\text{Ar}}{^{36}\text{Ar}}\right)_{1525 \text{ Ma}} = \left(\frac{^{40}\text{Ar}}{^{36}\text{Ar}}\right)_{1585 \text{ Ma}} + \left(\frac{[\text{K}]}{f \cdot [^{36}\text{Ar}]_{\text{initial}}} \times \frac{^{40}\text{K} \cdot \lambda_{\text{EC}}}{\text{K} \cdot \lambda_{\text{TOTAL}}} (e^{\lambda t_{1585 \text{ Ma}}} - e^{\lambda t_{1525 \text{ Ma}}})\right) \quad (1)$$

$$\left(\frac{^{40}\text{Ar}}{^{36}\text{Ar}}\right)_{1585 \text{ Ma}} = 296 + \left(\frac{[\text{K}]}{[^{36}\text{Ar}]_{\text{initial}}} \times \frac{^{40}\text{K} \cdot \lambda_{\text{EC}}}{\text{K} \cdot \lambda_{\text{TOTAL}}} (e^{\lambda t_{1870 \text{ Ma}}} - e^{\lambda t_{1585 \text{ Ma}}})\right) \quad (2)$$

where the whole rock initial ^{36}Ar concentration is assumed to be $5 \times 10^{-12} \text{ mol g}^{-1}$, that is toward the upper limit reported for sedimentary rocks [55], the K concentration is 3 wt.% ($7.7 \times 10^{-4} \text{ mol g}^{-1}$), the protolith has an age of 1870 Ma [4] and f (assumed to be 50–90%) equals the fraction of Ar lost during D_2 metamorphism at 1585 Ma [30].

Some involvement of metamorphic fluids is supported by the presence of CO_2 fluid inclusions that are inferred to have low (crustal) $^{40}\text{Ar}/^{36}\text{Ar}$ values (Fig. 3), and are equally abundant in all the samples irrespective of sample maximum $^{40}\text{Ar}/^{36}\text{Ar}$ value (Tables 1 and 2). However, devolatilisation of the Corella Formation is unlikely to have been the exclusive source of fluid #2, because such a fluid would have been even richer in

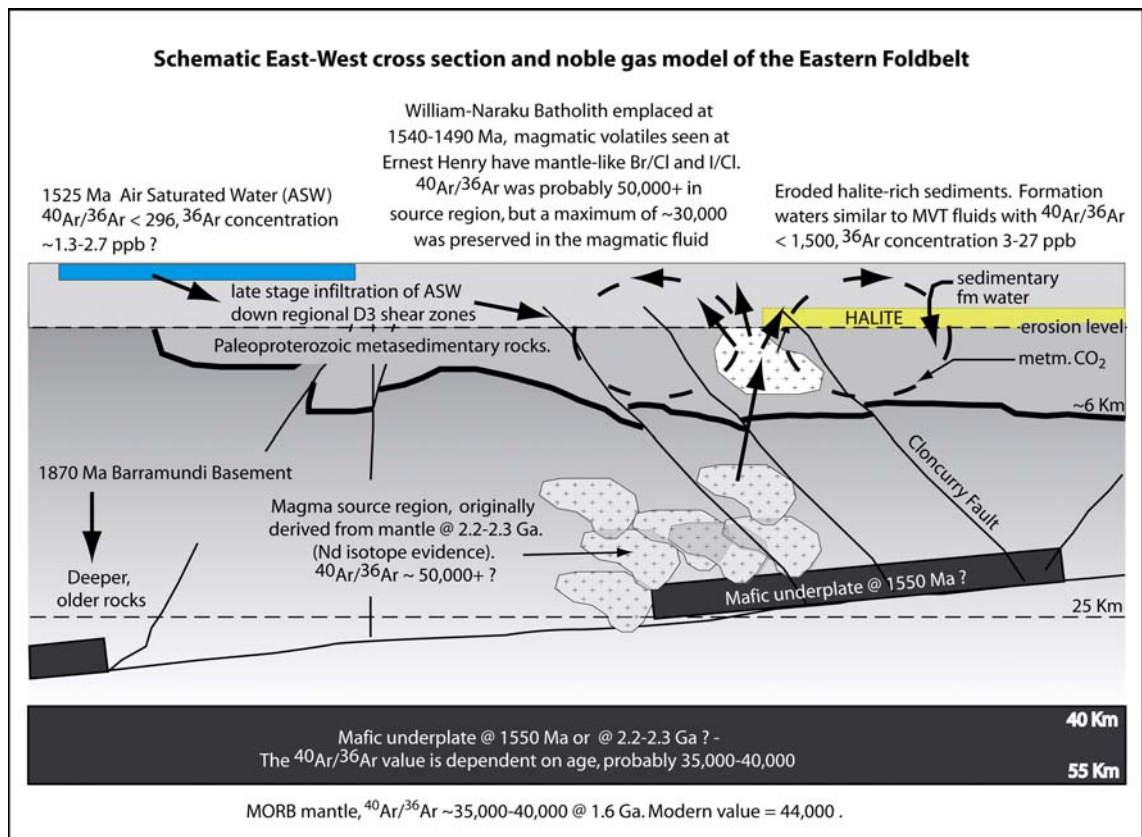


Fig. 7. Schematic crustal cross-section based on the Mt Isa seismic transect [40]. The range of fluid compositions in terms of both noble gases and halogens measured in primary fluid inclusions (Table 3) is most easily explained by convective circulation of magmatic fluids plus sedimentary formation waters with dissolution of halite and minor metamorphic devolatilisation. Later fluids in LV fluid inclusions are probably dominated by a surficial component. Sedimentary formation waters [20,21,50,53,68]; Nd and Hf isotope evidence for magma source region [4,35,37]; noble gas [55].

CO_2 than observed (Table 1; [65]). Furthermore, the stable isotope signature calculated for Ernest Henry ore fluids indicates an external fluid source from either magmatic or sedimentary formation waters [5,6]. The low ^{36}Ar concentrations determined for fluid #2 (Fig. 4; Table 3) are in the range expected for basement-derived metamorphic fluids [26] and are also compatible with fluids sourced from meta-sedimentary rocks that lost much of their Ar during peak metamorphism. However, the low ^{36}Ar concentrations could alternatively indicate that Ar was lost from fluid #2 during phase separation, even though the noble gas elemental ratios are unfractionated and do not preserve evidence for such a process (Table 2; Section 5.1).

Further work constraining the noble gas elemental ratios (F^{84}Kr and F^{129}Xe) of IOCG ore fluids in unirradiated samples, that are free of interfering fissionogenic isotopes, is required to constrain the potential significance of Ar-loss and noble gas fractionation during phase separation. In addition, direct

measurement of Br/Cl and I/Cl in meta-evaporitic scapolite of the Corella Formation will enable a fuller assessment of these rocks as a potential Cl-source.

5.3. Possible implications for Proterozoic mantle and seawater

It has been argued that the mantle-like Br/Cl composition of magmatic fluids is representative of their source region, and at Ernest Henry the ligands in fluid #1 were sourced from recycled Paleoproterozoic igneous rocks [4,34,35], but had an ultimately mantle origin (Section 5.1). If so, the similarity of Br/Cl in Proterozoic magmatic fluids at Ernest Henry, and Phanerozoic PCD (Fig. 6), indicates that the mantle has had a relatively constant Br/Cl composition through time, within the limits of $\sim 1-2 \times 10^{-3}$. This inference is compatible with the uniform Br/Cl composition of mantle fluids in diamonds of probable Archaean to Cretaceous age (but see Burgess et al., 2002 [57]).

In contrast, the most magmatic-like ore fluids at Ernest Henry have I/Cl values that are at the very lower limit of compositions recorded in either PCD fluids [22,23] or mantle fluids in diamond [49,57] (Fig. 6). This difference might be explained if PCD magmas (and some diamonds) are sourced from above subducting slabs that are enriched in I-rich sedimentary material, but Paleoproterozoic crust beneath the Mt Isa Inlier comprised igneous rocks derived from I-poor-mantle distal, or unrelated, to subducting slabs [4,34,35]. Alternatively, the Paleoproterozoic mantle source region may have been I-depleted relative to Phanerozoic mantle source-regions if I-rich organic material was not efficiently recycled into the mantle prior to ~ 2 Ga.

The above interpretation is speculative and requires further, more direct investigation of granite-related magmatic fluid compositions. However, it does demonstrate that the composition of paleo-fluids preserved in ore deposit fluid inclusions could have geochemical significance well beyond the genesis of the ore deposit. If correct, it is implied that because the mantle buffers seawater Br/Cl [57,59], the Br/Cl value of late Archaean to Paleoproterozoic seawater would have been similar to the modern day value of $\sim 1.5 \times 10^{-3}$, within the range of mantle fluids in diamond and some magmatic fluids ($\sim 1\text{--}2 \times 10^{-3}$) [23,49,57]. In contrast, the I/Cl values of both the mantle and seawater are more likely to have exhibited temporal variability.

6. Summary

The total inter- and intra-sample variability of Br/Cl, I/Cl, $^{40}\text{Ar}/^{36}\text{Ar}$, $^{40}\text{Ar}_E/\text{Cl}$ and ^{36}Ar concentration in IOCG ore fluids is interpreted to provide evidence for the involvement of high salinity deeply derived magmatic fluids and upper-crustal sedimentary formation waters. In addition, ‘locally derived’ mid-crustal metamorphic volatiles had some involvement and late secondary fluid inclusions preserve evidence for Air Saturated Water (Table 3; Fig. 7).

The magmatic fluid with a ^{36}Ar concentration of $\sim 3\text{--}6$ ppb, has mantle-like Br/Cl and I/Cl values, and $^{40}\text{Ar}/^{36}\text{Ar}$ values of $\sim 29,000$. These values were probably characteristic of the 25–30 km deep, mantle-derived igneous rocks, that were the main source of metaluminous ‘A-type’ granites in the Cloncurry District at $\sim 1540\text{--}1490$ Ma [4,34–36]. The presence of a magmatic fluid supports the ~ 1525 Ma Cu–Au mineralisation age that is synchronous with late-orogenic magmatism, but post-dates peak metamorphism [6,30].

The CO_2 fluid inclusions are inferred to have low $^{40}\text{Ar}/^{36}\text{Ar}$ values of < 2500 indicative of a predominantly

‘local’ crustal origin. As melts formed from Paleoproterozoic igneous rocks are unlikely to be CO_2 -rich, the common occurrence of CO_2 fluid inclusions is most easily explained by a (post-peak) metamorphic origin during regional magmatism and Na–Ca alteration.

Further work is required to understand the relative importance of mid-crustal meta-evaporitic scapolite vs. upper-crustal halite, as alternative sources of ligands in ore fluids with low $^{40}\text{Ar}/^{36}\text{Ar}$, Br/Cl and I/Cl values. In addition, it is unclear if low ^{36}Ar concentrations, in this fluid end-member (Fluid #2), are characteristic of metamorphic fluids [26], or indicative of minor ^{36}Ar loss during phase separation. However, it is possible that the heavy noble gases are not (strongly) fractionated between supercritical aqueous and carbonic fluids at crustal depths of 6–10 km.

Acknowledgments

This work was funded by the predictive mineral discovery Co-operative Research Centre (pmd*CRC) and is published with permission. Stan Szczepanski is thanked for technical assistance in the lab. Two anonymous reviewers and the associate editor Richard Carlson are thanked for their constructive and insightful comments that improved the focus of this manuscript.

Appendix A. Supplementary data

Supplementary data associated with this article can be found, in the online version, at [doi:10.1016/j.epsl.2006.12.032](https://doi.org/10.1016/j.epsl.2006.12.032).

References

- [1] P.J. Williams, Metalliferous economic geology of the Mt Isa Eastern Succession, Queensland, Aust. J. Earth Sci. 45 (1998) 329–341.
- [2] P.J. Williams, R.G. Skirrow, Overview of iron oxide–copper–gold deposits in the Curnamona Province and Cloncurry District (Eastern Mount Isa Block), Australia, in: T.M. Porter (Ed.), Hydrothermal Iron Oxide Copper–Gold and Related Deposits: A Global Perspective, vol. 1, PGC Publishing, Adelaide, 2000, pp. 105–122.
- [3] G. Mark, N.H.S. Oliver, M.J. Carew, Insights into the genesis and diversity of epigenetic Cu–Au mineralisation in the Cloncurry district, Mt Isa Inlier, northwest Queensland, Aust. J. Earth Sci. 53 (2006) 109–124.
- [4] R.W. Page, S.-S. Sun, Aspects of geochronology and crustal evolution in the Eastern Fold Belt, Mount Isa Inlier, Aust. J. Earth Sci. 45 (1998) 343–362.
- [5] G. Mark, N.S. Oliver, P.J. Williams, R.K. Valenta, R.A. Crookes, The evolution of the Ernest Henry Fe–Oxide–(Cu–Au) hydrothermal system, in: T.M. Porter (Ed.), Hydrothermal Iron Oxide Copper–Gold and Related Deposits: A Global Perspective, vol. 1, PGC Publishing, Adelaide, 2000, pp. 123–136, 1.

- [6] G. Mark, N.H.S. Oliver, P.J. Williams, Mineralogical and chemical evolution of the Ernest Henry Fe oxide–Cu–Au ore system, Cloncurry district, northwest Queensland, Australia, *Miner. Depos.* 40 (2006) 769–801.
- [7] M.W. Hitzmann, Iron oxide–Cu–Au deposits: what, where, when and why, in: T.M. Porter (Ed.), *Hydrothermal Iron Oxide Copper Gold and Related Deposits: A Global Perspective*, PGC Publishing, Adelaide, 2000, pp. 9–25.
- [8] M.D. Barton, D.A. Johnson, Evaporitic-source model for igneous related Fe oxide (REE–Cu–Au–U) mineralization, *Geology* 24 (1996) 259–262.
- [9] N.H.S. Oliver, J.S. Cleverley, G. Mark, P.J. Pollard, B. Fu, L.J. Marshall, M.J. Rubenach, P.J. Williams, T. Baker, Modeling the role of sodic alteration in the genesis of iron-oxide–copper–gold deposits, eastern Mt Isa block, Australia, *Econ. Geol.* 99 (2004) 1145–1176.
- [10] G. Mark, D.R.W. Foster, P.J. Pollard, P.J. Williams, J. Tolman, M. Darvall, K.L. Blake, Stable isotope evidence for magmatic fluid input during large-scale Na–Ca alteration in the Cloncurry Fe oxide Cu–Au district, NW Queensland, Australia, *Terra Nova* 16 (2004) 54–61.
- [11] M.A. Kendrick, T. Baker, B. Fu, D. Phillips, P.J. Williams Noble gas and halogen constraints on regionally extensive mid-crustal Na–Ca metasomatism, the Proterozoic Eastern Mt Isa Block, Australia, *Precambrian Res.* (in press).
- [12] G. Mark, A. Wilde, N.H.S. Oliver, P.J. Williams, C.G. Ryan, Modeling outflow from the Ernest Henry Fe oxide Cu–Au deposit: implications for ore genesis and exploration, *J. Geochem. Explor.* 85 (1) (2005) 31–46.
- [13] N. Adshead, P. Voulgaris, V.N. Muscio, Osborne copper–gold deposit, in: D.A. Berkman, D.H. MacKenzie (Eds.), *Geology of Australian and Papua New Guinean Mineral Deposits*, The Australian Institute of Mining and Metallurgy, Melbourne, 1998.
- [14] T. Baker, Alteration, mineralisation, and fluid evolution at the Eloise Cu–Au deposit, Cloncurry District, Northwest Queensland, Australia, *Econ. Geol.* 93 (1998) 1213–1236.
- [15] M.A. Kendrick, J.M. Miller, D. Phillips, Part I. Decrepitation and degassing behaviour of quartz up to 1560 C: analysis of noble gases and halogens in complex fluid inclusions assemblages, *Geochim. Cosmochim. Acta* 70 (2006) 2540–2561.
- [16] G. Xu, Fluid inclusions with NaCl–CaCl₂–H₂O composition from the Cloncurry hydrothermal system, NW Queensland, Australia, *Lithos* 53 (1) (2000) 21–35.
- [17] P.J. Pollard, Evidence of a magmatic fluid and metal source for Fe-oxide Cu–Au mineralisation, in: T.M. Porter (Ed.), *Hydrothermal Iron Oxide Copper Gold and Related Deposits: A Global Perspective*, PGC Publishing, Adelaide, 2000, pp. 27–41.
- [18] J.S. Hanor, Origin of saline fluids in sedimentary basins, in: J. Parnell (Ed.), *Geofluids: Origin, Migration and Evolution of Fluids in Sedimentary Basins*, Geological Society Special Publication, vol. 78, 1994, pp. 151–174.
- [19] W.T. Holser, Trace elements and isotopes in evaporites, in: R.G. Burns (Ed.), *Marine Minerals, Reviews in Mineralogy*, vol. 6, Mineralogical Society of America, Washington, D.C., 1979, pp. 295–346.
- [20] M.A. Kendrick, R. Burgess, R.A.D. Patrick, G. Turner, Hydrothermal fluid origins in a fluorite-rich Mississippi valley-type deposit: combined noble gas (He, Ar, Kr) and halogen (Cl, Br, I) analysis of fluid inclusions from the South Pennine Orefield, United Kingdom, *Econ. Geol.* 97 (3) (2002) 435–451.
- [21] M.A. Kendrick, R. Burgess, D. Leach, R.A.D. Patrick, Hydrothermal fluid origins in Mississippi valley-type ore deposits: combined noble gas (He, Ar, Kr) and halogen (Cl, Br, I) analysis of fluid inclusions from the Illinois–Kentucky Fluorspar district, Viburnum Trend, and Tri-State districts, mid-continent United States, *Econ. Geol.* 97 (3) (2002) 452–479.
- [22] J.J. Irwin, E. Roedder, Diverse origins of fluid inclusions at Bingham (Utah, USA), Butte (Montana, USA), St. Austell (Cornwall, UK) and Ascension Island (mid-Atlantic, UK), indicated by laser microprobe analysis of Cl, K, Br, I, Ba+Te, U, Ar, Kr, and Xe, *Geochim. Cosmochim. Acta* 59 (2) (1995) 295–312.
- [23] M.A. Kendrick, R. Burgess, R.A.D. Patrick, G. Turner, Noble gas and halogen evidence on the origin of Cu-Porphyry mineralising fluids, *Geochim. Cosmochim. Acta* 65 (2001) 2651–2668.
- [24] P. Burnard, D. Graham, G. Turner, Vesicle-specific noble gas analyses of “popping rock”; implications for primordial noble gases in the Earth, *Science* 276 (1997) 568–571.
- [25] M. Moriera, J. Kunz, C.J. Allegre, Rare gas systematics in popping rock: isotopic and elemental compositions in the upper mantle, *Science* 279 (1998) 1178–1181.
- [26] M.A. Kendrick, R.J. Duncan, D. Phillips, Noble gas and halogen constraints on mineralizing fluids of metamorphic versus surficial origin: Mt Isa, Australia, *Chem. Geol.* 235 (2006) 325–351.
- [27] G.N. Phillips, R. Powell, Link between Gold Provinces, *Econ. Geol.* 88 (1993) 1084–1098.
- [28] D.G. Bennett, A.J. Barker, High salinity fluids: the result of retrograde metamorphism in thrust zones, *Geochim. Cosmochim. Acta* 56 (1992) 81–95.
- [29] H. Svensen, D.A. Banks, H. Austrheim, Halogen contents of eclogite facies fluid inclusions and minerals: Caledonides, western Norway, *J. Metamorph. Geol.* 19 (2001) 165–178.
- [30] D.R.W. Foster, M.J. Rubenach, Isograd pattern and regional low pressure, high-temperature metamorphism of pelitic, mafic and calc-silicate rocks along an east-west section through the Mt Isa Inlier, *Aust. J. Earth Sci.* 53 (2006) 167–186.
- [31] D.H. Blake, Geology of the Mount Isa Inlier and environs, Queensland and Northern Territory, *Aust. Bur. Miner. Resour. Bull.* 255 (1987) 83.
- [32] L. Gauthier, G. Hall, H. Stein, U. Schaltegger, The Osborne deposit, Cloncurry District: a 1595 Ma Cu–Au Skarn deposit, in: P.J. Williams (Ed.), *A Hydrothermal Odyssey*, James Cook University, Townsville, 2001, pp. 58–59.
- [33] G. Mark, N. Phillips, P.J. Pollard, Highly selective partial melting of Pelitic gneiss at Cannington, Cloncurry district, Queensland, *Aust. J. Earth Sci.* 45 (1998) 169–176.
- [34] L.A.I. Wyborn, Younger ca 1500 Ma granites of the Williams and Naraku Batholiths, Cloncurry district, eastern Mt Isa Inlier: geochemistry, origin, metallogenic significance and exploration indicators, *Aust. J. Earth Sci.* 45 (1998) 397–411.
- [35] G. Mark, Nd isotope and petrogenetic constraints for the origin of the Mount Angelay igneous complex: implications for the origin of intrusions in the Cloncurry district, NE Australia, *Precambrian Res.* 105 (2001) 17–35.
- [36] L.A.I. Wyborn, R.W. Page, M.T. McCulloch, Petrology, geochronology, and isotope geochemistry of the post-1820 Ma granites of the Mt Isa Inlier: mechanisms for the generation of Proterozoic anorogenic granites, in: L.A.I. Wyborn, M.A. Etheridge (Eds.), *The Early to Middle Proterozoic of Australia*, *Precambrian Research*, vol. 40/41, 1988, pp. 509–541.
- [37] W.L. Griffin, E.A. Belousova, S.G. Walters, S.Y. O’Reilly, Archaean and Proterozoic crustal evolution in the Eastern

- Succession of the Mt Isa district, Australia: U–Pb and Hf-isotope studies of detrital zircons, *Aust. J. Earth Sci.* 53 (2006) 125–149.
- [38] G. Mark, Petrogenesis of Mesoproterozoic K-rich granitoids, southern Mt Angelay igneous complex, Cloncurry district, northwest Queensland, *Aust. J. Earth Sci.* 46 (1999) 933–949.
- [39] P.J. Pollard, G. Mark, L.C. Mitchell, Geochemistry of post-1540 Ma granites in the Cloncurry District, Northwest Queensland, *Econ. Geol.* 93 (1998) 1330–1344.
- [40] T. MacCready, B.R. Goleby, A. Goncharov, B.J. Drummond, G.S. Lister, A framework of overprinting orogens based on interpretation of the Mt Isa deep seismic transect, *Econ. Geol.* 93 (1998) 1422–1434.
- [41] G. de Jong, P.J. Williams, Giant metasomatic system formed during exhumation of mid crustal Proterozoic rocks in the vicinity of the Cloncurry fault, northwest Queensland, *Aust. J. Earth Sci.* 42 (1995) 281–290.
- [42] M.J. Rubenach, K.A. Lewthwaite, Metasomatic albitites and related biotite schists from a low-pressure polymetamorphic terrane, Snake Creek Anticline, Mount Isa Inlier, north-eastern Australia: microstructures and P–T–d paths, *J. Metamorph. Geol.* 20 (2002) 191–202.
- [43] M.J. Rubenach, A.J. Barker, Metamorphic and metasomatic evolution of the Snake Creek Anticline, Eastern Succession, Mount Isa Inlier, *Aust. J. Earth Sci.* 45 (1998) 363–372.
- [44] M.J. Rubenach, D.A. Foster, P.M. Evins, K.L. Blake, C.M. Fanning, Age constraints on the tectonothermal evolution of the Selwyn Zone, Eastern Fold Belt, Mt Isa Inlier, *Precambrian Res.* (in press).
- [45] C.S. Perring, P.J. Pollard, G. Dong, A.J. Nunn, K.L. Blake, The Lightning Creek Sill Complex, Cloncurry District, Northwest Queensland: a source of fluids for Fe oxide Cu–Au mineralisation and sodic–calcic alteration, *Econ. Geol.* 95 (2000) 1067–1089.
- [46] J.F. Rotherham, K.L. Blake, I. Cartwright, P.J. Williams, Stable isotope evidence for the origin of the mesoproterozoic Starra Au–Cu deposit, Cloncurry District, Northwest Queensland, *Econ. Geol.* 93 (1998) 1435–1449.
- [47] J.C. Roddick, High precision intercalibration of 40Ar–39Ar standards, *Geochim. Cosmochim. Acta* 47 (1983) 887–898.
- [48] I. McDougall, T.M. Harrison, *Geochronology and Thermochronology by the 40Ar/39Ar Method*, Oxford University Press, Oxford, New York, 1999, 269 pp.
- [49] L.H. Johnson, R. Burgess, G. Turner, H.J. Milledge, J.W. Harris, Noble gas and halogen geochemistry of mantle diamonds: comparison of African and Canadian diamonds, *Geochim. Cosmochim. Acta* 64 (2000) 717–732.
- [50] S. Kelley, G. Turner, A.W. Butterfield, T.J. Shepherd, The source and significance of argon isotopes in fluid inclusions from areas of mineralization, *Earth Planet. Sci. Lett.* 79 (1986) 303–318.
- [51] M.A. Kendrick, R. Burgess, R.A.D. Patrick, G. Turner, Halogen and Ar–Ar age determinations of inclusions within quartz veins from porphyry copper deposits using complementary noble gas extraction techniques, *Chem. Geol.* 177 (2001) 351–370.
- [52] M.A. Kendrick, J.M. Miller, D. Phillips, Part II: Evaluation of 40Ar–39Ar quartz ages: implications for fluid inclusion retentivity and determination of initial 40Ar/36Ar values in Proterozoic samples, *Geochim. Cosmochim. Acta* 70 (2006) 2562–2576.
- [53] G. Turner, M.P. Bannon, Argon isotope geochemistry of inclusion fluids from granite-associated mineral veins in southwest and northeast England, *Geochim. Cosmochim. Acta* 56 (1992) 227–243.
- [54] M.A. Kendrick, Comment on ‘Palaeozoic ages and excess 40Ar in garnets from the Bixiling eclogite in Dabieshan, China: new insights from 40Ar/39Ar dating by stepwise crushing by Hua-Ning Qiu and J.R. Wijbrans’, *Geochim. Cosmochim. Acta.* (in press).
- [55] M. Ozima, F.A. Podosek, *Noble Gas Geochemistry*, Cambridge University Press, 2002.
- [56] J. Drescher, T. Kirsten, K. Schäfer, The rare gas inventory of the continental crust, recovered by the KTB Continental Deep Drilling Project, *Earth Planet. Sci. Lett.* 154 (1998) 247–263.
- [57] R. Burgess, E. Layzelle, G. Turner, J.W. Harris, Constraints on the age and halogen composition of mantle fluids in Siberian coated diamonds, *Earth Planet. Sci. Lett.* 197 (3–4) (2002) 193–203.
- [58] C.A. Heinrich, J.H.C. Bain, J.J. Fardy, C.L. Waring, Br/Cl geochemistry of hydrothermal brines associated with Proterozoic metasediment-hosted copper mineralization at Mount Isa, northern Australia, *Geochim. Cosmochim. Acta* 57 (1993) 2991–3000.
- [59] J.G. Schilling, C.K. Unni, M.L. Bender, Origin of chlorine and bromine in the oceans, *Nature* 273 (1978) 631–635.
- [60] B.W.D. Yardley, D.A. Banks, I.A. Munz, Halogen compositions of fluid inclusions as tracers of crustal fluid behaviour, in: Kharaka, Maest (Eds.), *Water–Rock Interaction*, Balkema, Rotterdam, 1992, pp. 1137–1140.
- [61] D.A. Banks, R. Green, R.A. Cliff, B.W.D. Yardley, Chlorine isotopes in fluid inclusions: determination of the origins of salinity in magmatic fluids, *Geochim. Cosmochim. Acta* 64 (2000) 1785–1789.
- [62] P.J. Pollard, Sodic–(calcic) alteration in Fe-oxide–Cu–Au districts: and origin via unmixing of magmatic H₂O–CO₂–NaCl+/-CaCl₂–KCl fluids, *Miner. Depos.* 36 (2001) 93–100.
- [63] M. Chiaradia, D. Banks, R.A. Cliff, R. Marschik, A. de Haller, Origin of fluids in iron oxide–copper–gold deposits: constraints from d37Cl, 87Sr/86Sr and Cl/Br, *Miner. Depos.* 41 (2006) 565–573.
- [64] Y. Pan, P. Dong, Bromine in scapolite-group minerals and sodalite: XRF microprobe analysis, exchange experiments, and application to skarn deposits, *Can. Mineral.* 41 (2003) 529–540.
- [65] N.H.S. Oliver, V.J. Wall, I. Cartwright, Internal control of fluid composition in amphibolite-facies scapolitic calc-silicate rocks, Mary Kathleen, Australia, *Contrib. Mineral. Petrol.* 111 (1992) 94–112.
- [66] I.K. Zherebtsova, N.N. Volkova, Experimental study of behaviour of trace elements in the process of natural solar evaporation of Black Sea water and Lake Sasyk-Sivash brine, *Geochem. Int.* 3 (1966) 656–670.
- [67] J.Ch. Fontes, J.M. Matray, Geochemistry and origin of formation brines from the Paris Basin, France 1. Brines associated with Triassic salts, *Chem. Geol.* 109 (1993) 149–175.
- [68] J.K. Böhlke, J.J. Irwin, Brine history indicated by argon, krypton, chlorine, bromine, and iodine analyses of fluid inclusions from the Mississippi Valley type lead–fluorite–barite deposits at Hansonburg, New Mexico, *Earth Planet. Sci. Lett.* 110 (1992) 51–66.